

# Three-jet event-shapes in lepton-proton scattering at next-to-leading order accuracy

Zoltán Nagy<sup>a</sup> and Zoltán Trócsányi<sup>b</sup>

<sup>a</sup>*University of Zürich, Winterthurerstrasse 190, CH-857 Zürich, Switzerland*

<sup>b</sup>*University of Debrecen and Institute of Nuclear Research of the Hungarian Academy of Sciences, H-4001 Debrecen P.O.Box 51, Hungary*

---

## Abstract

We compute the differential distributions of two three-jet event-shape observables at the next-to-leading order accuracy at fixed values of the DIS kinematic variables. The observable  $K_{\text{out}}$  measures the out-of-event-plane momentum. The other observable  $y_3$  is the maximum value of the  $y_{\text{cut}}$  resolution variable for which an event is classified as three-jet event. We also show the dependence of the fixed-order predictions on the renormalization and factorization scales. The radiative corrections are in general large and depend on the value of the DIS kinematic range.

*Key words:* perturbative QCD, deep-inelastic scattering, event shapes

*PACS:* 12.38Bx, 13.60.Hb, 13.87.Ce

---

## 1 Introduction

The analysis of event-shape observables in  $e^+e^-$ -annihilation and in deeply-inelastic lepton-proton scattering (DIS) proved to be a powerful method to study Quantum Chromodynamics (QCD) [1]. The standard QCD analysis of event-shapes consists of matching the next-to-leading order (NLO) and resummed next-to-leading logarithmic (NLL) predictions, possibly improved with analytic predictions for the power corrections (PC). Such matched predictions also describe the distributions of multi-jet rates in  $e^+e^-$  annihilation with high accuracy [2]. Thus, it is interesting to investigate whether similar level of accuracy can also be achieved in predicting distributions of multi-jet observables in DIS.

Two-jet<sup>1</sup> event-shape observables in DIS have been thoroughly analyzed both

---

<sup>1</sup> In counting the number of jets in this paper, we neglect the ubiquitous beam-jet.

theoretically [3] and experimentally [4]. Three-jet rates have been also analyzed [5] based on computations valid at the NLO accuracy [6]. Resummed prediction to the three-jet rates have not yet been computed, therefore matched predictions are not available for jet rates. However, much progress has been achieved in computing resummed predictions at the NLL accuracy for three-jet event shapes [7,8,9] that are sensitive to large angle soft emission and thus exhibit rich geometry-dependent structure. These developments in theory encouraged the experimenters to consider three-jet event shapes [10]. However, predictions to three-jet event shapes at the NLO accuracy have not been computed yet. In this letter we aim to fill this gap.

It is well-known that the validity of fixed-order predictions is rather constrained. In the perturbative expansion of the distribution of an observable  $O$ , logarithmic terms  $\alpha_s^m \log^n O$  appear which require all-order resummation if the value of  $O$  is small. In analyzing the data, most of the statistics lie in the range of small  $O$ , thus the computation of resummed predictions is indispensable for the experimental analysis. The observables we choose to compute are those for which resummed predictions are known.

The first three-jet event-shape observable in DIS that has been computed at the NLL accuracy is the  $K_{\text{out}}$  variable, that measures the out-of-event-plane QCD radiation. The observable  $K_{\text{out}}$  was defined in Ref. [7] as the sum of the momentum components perpendicular to the event plane,

$$K_{\text{out}} = \sum_h |p_h^{\text{out}}|. \quad (1)$$

The summation extends over all particles (hadrons in the experiment, partons in the theoretical computation). The event plane is spanned by the proton three-momentum  $\vec{p}$  and the unit vector  $\vec{n}$  that defines the thrust major axis in the plane perpendicular to the beam,

$$T_M = \max_{\vec{n}} \frac{1}{Q} \sum_h |\vec{p}_h \cdot \vec{n}|, \quad \vec{n} \cdot \vec{p} = 0. \quad (2)$$

Recently the CAESAR program has been published [8,9] that can be used for computing cross sections of two- and three-jet event shapes<sup>2</sup> in an automatic way. In particular, the distribution of the  $y_3$  observable, that is defined to be the largest value of the jet resolution variable  $y_{\text{cut}}$  such that the event is clustered into three jets, is also known to NLL accuracy [9]. For defining the jets, the computation uses the  $k_{\perp}$ -clustering algorithm of Ref. [11].

In this paper we compute the distributions of the two three-jet event shape

---

<sup>2</sup> It can also be used for computing dijet event shapes in hadronic collisions.

observables in DIS for which resummed predictions already exist, but the fixed-order radiative corrections have not been computed before. We use the NLOJET++ program [12].

## 2 Computation of fixed-order predictions

The next-to-leading order cross section for electron-proton scattering into three jets is the convolution of the parton density function of the incoming proton and the hard scattering cross section,

$$\sigma(p, q) = \sum_a \int_0^1 d\eta f_{a/P}(\eta, \mu_F^2) \left[ \sigma_a^{\text{LO}}(\eta p, q) + \sigma_a^{\text{NLO}}(\eta p, q) \right], \quad (3)$$

where  $p^\mu$  and  $q^\mu$  are the four-momenta of the incoming proton and the exchanged virtual photon, respectively,  $f_{a/P}(\eta, \mu_F^2)$  is the density of the parton of type  $a$  in the incoming proton at momentum fraction  $\eta$  and factorization scale  $\mu_F$ . The corresponding parton level cross sections are

$$\sigma_a^{\text{LO}}(p, q) \equiv \int_3 d\sigma_a^{\text{B}}(p, q) = \int_3 d\Gamma^{(3)} \langle |M_a^{(3)}|^2 \rangle J^{(3)}, \quad (4)$$

and the next-to-leading order correction is sum of three terms

$$\begin{aligned} \sigma_a^{\text{NLO}}(p, q) &\equiv \int d\sigma_a^{\text{NLO}}(p, q) \\ &= \int_4 d\sigma_a^{\text{R}}(p, q) + \int_3 d\sigma_a^{\text{V}}(p, q) + \int_3 d\sigma_a^{\text{C}}(p, q), \end{aligned} \quad (5)$$

where  $d\sigma^{\text{R}}$  and  $d\sigma^{\text{V}}$  are the real and virtual contributions to the partonic cross section. The contribution  $d\sigma^{\text{C}}$  represents the collinear-subtraction counter term. The pole structure of this term is unique, while its finite part depends on the factorization scheme. We use the  $\overline{\text{MS}}$  scheme as defined precisely in Ref. [13]. The parton density functions are also scheme dependent, so that the scheme-dependence cancels in the hadronic cross section of Eq. (3).

The three integrals on the right hand side of Eq. (5) are separately divergent but their sum is finite provided the jet function  $J^{(m)}$  defines a collinear and infrared safe quantity, which formally means that

$$J^{(4)} \longrightarrow J^{(3)}, \quad (6)$$

whenever the four-parton and three-parton configurations are kinematically degenerate (regions of one unresolved parton). In addition, to define a three-jet observable, both  $J^{(4)}$  and  $J^{(3)}$  have to vanish if less than three partons are resolved. The presence of the singularities means that the separate pieces have to be regularized and the divergences have to be cancelled. We use dimensional regularization in  $d = 4 - 2\varepsilon$  dimensions in which case the divergences are replaced by double and single poles of the form  $1/\varepsilon^2$  and  $1/\varepsilon$ . We assume that ultraviolet renormalization of all Green functions to one-loop order has been carried out, so the divergences are of infrared origin. In order to get the finite sum one has to rearrange the various contributions by subtracting and adding the same, in  $d = 4$  dimensions singular terms to the three contributions in Eq. (5) so that each becomes separately finite in  $d = 4$  dimensions.

The essence of this rearrangement is to define a single subtraction term  $d\sigma^A$  that regularizes the divergences in the real term which comes from the unresolved soft and collinear regions. Thus, the three singular integrals in Eq. (5) are substituted by three finite ones:

$$\sigma_a^{\text{NLO}}(p, q) = \sigma_a^{\text{NLO}\{4\}}(p, q) + \sigma_a^{\text{NLO}\{3\}}(p, q) + \int_0^1 dx \hat{\sigma}_a^{\text{NLO}\{3\}}(x, xp, q), \quad (7)$$

where the four-parton integral is given by

$$\sigma_a^{\text{NLO}\{4\}}(p, q) = \int_4 \left[ d\sigma_a^{\text{R}}(p, q)_{\varepsilon=0} - d\sigma_a^{\text{A}}(p, q)_{\varepsilon=0} \right]. \quad (8)$$

We have two three-parton contributions to the NLO correction. The second term on the right hand side of Eq. (7) is the sum of the one-loop contribution and a Born term convoluted with a universal singular factor  $\mathbf{I}$ ,

$$\sigma_a^{\text{NLO}\{3\}}(p, q) = \int_3 \left[ d\sigma_a^{\text{V}}(p, q) + d\sigma_a^{\text{B}}(p, q) \otimes \mathbf{I} \right]_{\varepsilon=0}. \quad (9)$$

The factor  $\mathbf{I}$  contains all the  $\varepsilon$  poles which come from the  $d\sigma^A$  and  $d\sigma^C$  terms that are necessary to cancel the (equal and with opposite sign) poles in  $d\sigma^V$ . The  $\otimes$  operation means correlations in colour space. The last term in Eq. (7) is a finite remainder, in the form of a convolution, that is left after factorization of initial-state collinear singularities into the non-perturbative parton distribution functions,

$$\int_0^1 dx \hat{\sigma}_a^{\text{NLO}\{3\}}(x, xp, q) =$$

$$\sum_{a'} \int_0^1 dx \int_3 \left[ d\sigma_{a'}^B(xp, q) \otimes [\mathbf{P}(x) + \mathbf{K}(x)]^{aa'} \right]_{\varepsilon=0}, \quad (10)$$

where the  $x$ -dependent functions  $\mathbf{P}$  and  $\mathbf{K}$  are similar (but finite for  $\varepsilon \rightarrow 0$ ) to the factor  $\mathbf{I}$ . These functions are universal, that is, they are independent of the scattering process and of the jet observables.

There are many ways to define the  $d\sigma^A$  subtraction term, but all must lead to the same finite next-to-leading order correction. In computing the NLO corrections to multijet cross sections the dipole subtraction scheme of Catani and Seymour [13] is a convenient formalism. It is used both in the DISENT and the NLOJET++ programs. The subtraction scheme applied in the NLOJET++ program is modified slightly as compared to the original one in [13] in order to have a better control on the numerical computation. The main idea is to cut the phase space of the dipole subtraction terms as introduced in Ref. [14]. We thus define the  $d\sigma^A$  local counter term as

$$\begin{aligned} d\sigma_a^A = & \sum_{\{4\}} d\Gamma^{(4)}(p_a, q, p_1, \dots, p_4) \frac{1}{S_{\{4\}}} \\ & \times \left\{ \sum_{\substack{\text{pairs} \\ i,j}} \sum_{k \neq i,j} D_{ij,k}(p_a, q, p_1, \dots, p_4) J^{(3)}(p_a, \dots, \tilde{p}_{ij}, \tilde{p}_k, \dots) \Theta(y_{ij,k} < \alpha) \right. \\ & + \sum_{\substack{\text{pairs} \\ i,j}} D_{ij}^a(p_a, q, p_1, \dots, p_4) J^{(3)}(\tilde{p}_a, \dots, \tilde{p}_{ij}, \dots) \Theta(1 - x_{ij,a} < \alpha) \\ & \left. + \sum_{i \neq k} D_k^{ai}(p_a, q, p_1, \dots, p_4) J^{(3)}(\tilde{p}_a, \dots, \tilde{p}_k, \dots) \Theta(u_i < \alpha) \right\}, \quad (11) \end{aligned}$$

where  $d\Gamma^{(4)}$  is the four-parton phase space including all the factors that are QCD independent,  $\sum_{\{4\}}$  denotes the sum over all configurations with 4 partons and  $S_{\{4\}}$  is the Bose symmetry factor of the identical partons in the final state. The  $D_{ij,k}$ ,  $D_{ij}^a$  and  $D_k^{ai}$  functions are the dipole factors given in Ref. [13]. The function  $J^{(3)}$  is the jet function which acts over the three-parton dipole phase space. The variables  $y_{ij,k}$ ,  $x_{ij,a}$  and  $u_i$  are the dipole variables used for defining the exact factorization of the phase space [13]. The parameter  $\alpha \in (0, 1]$  controls the volume of the dipole phase space. The case of  $\alpha = 1$  means the full dipole subtraction. We can speed up the computer program by choosing  $\alpha \simeq 0.1$ , which keeps the subtraction in the vicinity of the singular regions, but avoids the CPU-intensive computations of the dipole terms where those are not necessary. Furthermore, checking that the predictions are independent of the parameter  $\alpha$ , that sets the volume of the cut dipole phase space, gives a strong control that indeed the same quantity is subtracted from the real correction as added to the virtual one. Choosing  $\alpha < 1$ , the insertion operators  $\mathbf{I}(\alpha, \varepsilon)$ ,  $\mathbf{P}(\alpha)$ ,  $\mathbf{K}(\alpha)$  depend on  $\alpha$ . The explicit expressions can be found in Ref. [15].

The integrand of the NLO contribution  $\sigma_a^{\text{NLO}\{4\}}$  in Eq. (8) contains integrable square root singularities. Integrating these singularities by simple Monte Carlo integration technique (choosing random values of the integration variables uniformly) is not efficient because the variance of the estimate of the integral is formally infinite, therefore, the estimate of the statistical error of the integral is unreliable. To improve the convergence of the Monte Carlo integral, in the NLOJET++ program the phase space is generated by multi-channel weighted phase space generator [16].

Once the phase space integrations are carried out, we write the NLO jet cross section in the following form:

$$\sigma^{(J)} = \sum_a \int_0^1 d\eta f_{a/P}(\eta, \mu_F^2) \sigma_{a,\text{NLO}}^{(J)}(p_a, q, \alpha_s(\mu_R^2), \mu_R^2/Q_{\text{H.S.}}^2, \mu_F^2/Q_{\text{H.S.}}^2), \quad (12)$$

where  $\sigma_{a,\text{NLO}}^{(J)}$  represents the sum of the LO and NLO contributions to the partonic cross section, given in Eqs. (4) and (7) respectively, with jet function  $J$ . In addition to the parton momenta and possible parameters of the jet function, it also depends explicitly on the renormalized strong coupling  $\alpha_s(\mu_R^2)$ , the renormalization and factorization scales  $\mu_R = x_R Q_{\text{H.S.}}$  and  $\mu_F = x_F Q_{\text{H.S.}}$ , where  $Q_{\text{H.S.}}$  is the hard scale that characterizes the parton scattering. The scale  $Q_{\text{H.S.}}$  is usually set event by event to a measurable energy scale of the event. Furthermore, the cross section also depends on the electromagnetic coupling, for which we used  $\overline{\text{MS}}$  running  $\alpha_{\text{EM}}(Q^2)$  at the scale of the virtual photon momentum squared,  $Q^2 = -q^2$ .

The publicly available version of the NLOJET++ program [12] is based on the tree-level and one-loop matrix elements given in Refs. [14,17], crossed into the photon-parton channel. It uses a C/C++ implementation of the LHAPDF library [18] with CTEQ6 [19] parton distribution functions and with the corresponding  $\alpha_s$  expression for the renormalized coupling which is included in this library. The CTEQ6 set was fitted using the two-loop running coupling with  $\alpha_s(M_{Z^0}) = 0.118$ .

### 3 Results

We computed the distributions for fixed values of the DIS kinematic variables  $Q^2$  and  $x_B$ , as done in the resummation computations [9]. We used three sets of values:  $Q^2 = (35 \text{ GeV})^2$  with  $x_B = 0.02$  and  $0.2$  and  $Q^2 = (65 \text{ GeV})^2$  with  $x_B = 0.2$ . The  $Q^2 = (65 \text{ GeV})^2$  with  $x_B = 0.02$  kinematical point is not accessible at HERA. In order to select events with at least two jets with high transverse momenta ( $p_{\perp} \sim Q$ ), we required  $y_2 > 0.1$ , where  $y_2$  is the maximum

value of the jet resolution variable  $y_{\text{cut}}$  such that the event can be classified as a two-jet one [7]. We employed a cut on the rapidity of the final-state momenta in the Breit frame such that

$$\eta_i = \frac{1}{2} \ln \left( 1 + \frac{q \cdot p_i}{x_B p \cdot p_i} \right) < 3. \quad (13)$$

Figs. 1 and 2 show the differential distributions for  $K_{\text{out}}$  and  $y_3$  observables. The shaded bands correspond to the range of scales  $1/2 \leq x_\mu \leq 2$ , where  $x_\mu^2 = \mu_R^2/Q_{\text{H.S.}}^2 = \mu_F^2/Q_{\text{H.S.}}^2$ , with hard scattering scale chosen to be  $Q_{\text{H.S.}}^2 = Q^2$ . We observe several features of these plots.

Let us consider first the distributions in  $K_{\text{out}}$ . We find that the radiative corrections are in general large, thus the scale-dependence reduces only relatively to the cross sections. The corrections also depend strongly on the values of the DIS kinematic variables: they increase with decreasing  $Q^2$  and with decreasing  $x_B$  (as seen from the plots in the right panel). They also increase with increasing value of  $K_{\text{out}}$  because the phase space for events with large out-of-plane radiation with three partons in the final state (at LO) is much smaller than that with four partons in the final state (real corrections). The boundary of the phase space in  $K_{\text{out}}$  depends on the value of  $x_B$ , increases with decreasing  $x_B$ , and is about 20% larger for the NLO computation than at LO. The cross sections decrease rapidly with increasing  $K_{\text{out}}$ . The rate of this decrease also depends on  $x_B$ , being much quicker for larger values of  $x_B$  due to the smaller phase space. Nevertheless, the small cross section for medium or large values of  $K_{\text{out}}$  leaves the small  $K_{\text{out}}$ -region for experimental analysis.

In the small  $K_{\text{out}}$ -region, the logarithmic contributions of the type  $\ln K_{\text{out}}/Q$  are dominant as can be seen on the plots in the right panel. At LO, the cross section behaves as  $-\alpha_s(Q) \ln K_{\text{out}}/Q$ , while at NLO the asymptotically leading term is  $\alpha_s^2(Q) \ln^3 K_{\text{out}}/Q$  for small values of  $K_{\text{out}}$ , therefore, the fixed-order predictions diverge with  $K_{\text{out}} \rightarrow 0$  with alternating signs, which makes the resummation of these large logarithmic contributions mandatory. Reliable theoretical predictions can be obtained by matching the cross sections valid at the NLO and NLL accuracy as described in Ref. [20,3].

Similar qualitative conclusions can be drawn from the  $y_3$  distributions with some important differences. Although the corrections are also large, they are much smaller than in the case of the  $K_{\text{out}}$ . Thus the reduction in the scale-dependence can clearly be seen. An important reason for the smaller corrections is that the phase space in  $y_3$  is the same at LO as at NLO. The size of the corrections depends more on the value of the momentum transfer, less on  $x_B$ . However, the phase space in  $y_3$  is more dependent on  $x_B$  (increases with decreasing  $x_B$ ), than on  $Q^2$  (decreases slightly with increasing  $Q^2$ ). The cross section is sizable again for small values of the event shape and the need for

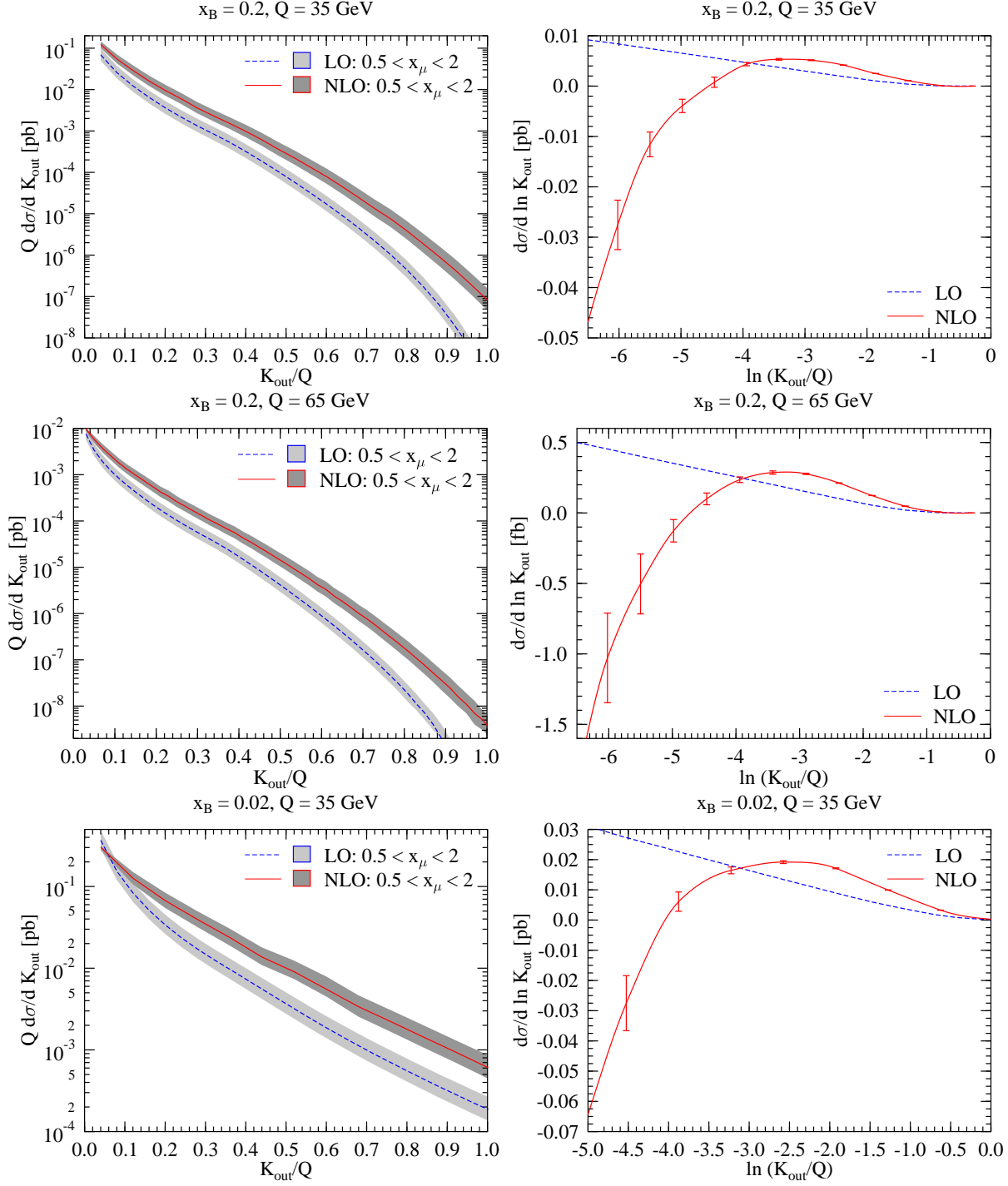


Fig. 1. The differential distribution of the  $K_{\text{out}}$  observable at three different fixed values of the DIS kinematic variables. The left panel shows the distributions as a function of  $K_{\text{out}}/Q$ , the right panel shows the distributions as a function of  $\ln K_{\text{out}}/Q$  in order to exhibit the logarithmic dominance for small values of the observable. The LO predictions are shown with dashed lines, the NLO predictions are shown with solid lines. The errorbars indicate the uncertainty of the numerical integration that is negligible for the computation at LO accuracy.



resummation in this region is clearly seen on the right panel.

## 4 Conclusions

In this paper we presented a computation of NLO corrections to the differential distributions of the three-jet event-shape observables  $K_{\text{out}}$  and  $y_3$  in DIS. We found large radiative corrections, especially in the case of  $K_{\text{out}}$ , indicating that the inclusion of even higher order corrections as well as the non-perturbative power corrections is necessary in order to make a reliable prediction, useful for experimental analysis. The cross sections decrease rapidly with increasing values of the event-shape variables, leaving the region of small values of the observables with sufficient statistics for an experimental analysis of data collected at HERA. In these regions the all-order resummed predictions in the NLL approximation are known, therefore, the matching of the NLO and NLL distributions promises us reliable predictions. Such results are expected to be available soon [21].

We are grateful to G. Zanderighi and A. Banfi for their helpful correspondence on DIS event-shape observables. This work was supported by the Hungarian Scientific Research Fund grant OTKA T-038240 and by the Swiss National Science Foundation (SNF) under contract number 200020-109162.

## References

- [1] M. Dasgupta and G. P. Salam, *J. Phys. G* **30**, R143 (2004) [arXiv:hep-ph/0312283].
- [2] Z. Nagy and Z. Trócsányi, *Nucl. Phys. Proc. Suppl.* **74**, 44 (1999) [hep-ph/9808364].
- [3] M. Dasgupta and G. P. Salam, *JHEP* **0208**, 032 (2002) [arXiv:hep-ph/0208073].
- [4] C. Adloff *et al.* [H1 Collaboration], *Eur. Phys. J. C* **14**, 255 (2000) [Erratum-*ibid.* C **18**, 417 (2000)] [arXiv:hep-ex/9912052];  
S. Chekanov *et al.* [ZEUS Collaboration], *Eur. Phys. J. C* **27**, 531 (2003) [arXiv:hep-ex/0211040].
- [5] C. Adloff *et al.* [H1 Collaboration], *Phys. Lett. B* **515**, 17 (2001) [arXiv:hep-ex/0106078];  
S. Chekanov *et al.* [ZEUS Collaboration], arXiv:hep-ex/0502007.
- [6] Z. Nagy and Z. Trócsányi, *Phys. Rev. Lett.* **87**, 082001 (2001) [arXiv:hep-ph/0104315];

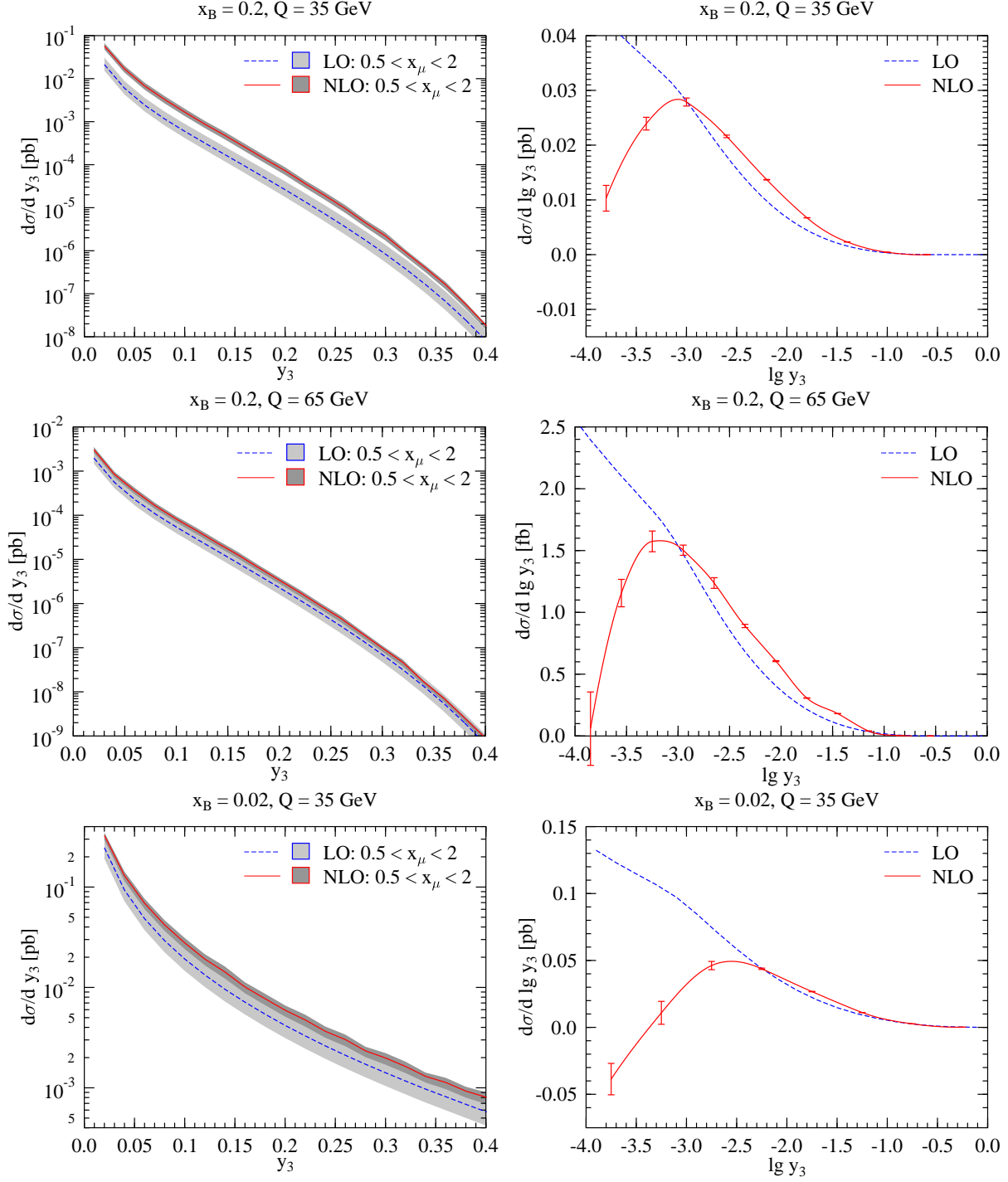


Fig. 2. The differential distribution of the  $y_3$  observable at three different fixed values of the DIS kinematic variables. The left panel shows the distributions as a function of  $y_3$ , the right panel shows the distributions as a function of  $\lg y_3 \equiv \log_{10} y_3$  in order to exhibit the logarithmic dominance for small values of the observable. The LO predictions are shown with dashed lines, the NLO predictions are shown with solid lines. The errorbars indicate the uncertainty of the numerical integration that is negligible for the computation at LO accuracy.

- [7] A. Banfi, G. Marchesini, G. Smye and G. Zanderighi, *JHEP* **0111**, 066 (2001) [arXiv:hep-ph/0111157].
- [8] A. Banfi, G. P. Salam and G. Zanderighi, *JHEP* **0503**, 073 (2005) [arXiv:hep-ph/0407286].
- [9] A. Banfi, G. P. Salam and G. Zanderighi, CAESAR homepage: qcd-caesar.org.
- [10] A. Everett, “Event shapes in deep inelastic  $ep \rightarrow eX$  scattering at HERA”, Proceedings of the XIII International Workshop on Deep Inelastic Scattering.
- [11] S. Catani, Y. L. Dokshitzer and B. R. Webber, *Phys. Lett. B* **285**, 291 (1992).
- [12] Z. Nagy, NLOJET++ homepage: www.cpt.dur.ac.uk/~nagy/nlo++/.
- [13] S. Catani and M. H. Seymour, *Nucl. Phys. B* **485**, 291 (1997) [Erratum-ibid. B **510**, 291 (1997)] [hep-ph/9605323].
- [14] Z. Nagy and Z. Trócsányi, *Phys. Rev. D* **59**, 014020 (1999) [Erratum-ibid. D **62**, 014020 (1999)] [hep-ph/9806317].
- [15] Z. Nagy, *Phys. Rev. D* **68**, 094002 (2003) [arXiv:hep-ph/0307268].
- [16] R. Kleiss and R. Pittau, *Comput. Phys. Commun.* **83**, 141 (1994) [arXiv:hep-ph/9405257].
- [17] Z. Bern, L. Dixon, D. A. Kosower and S. Weinzierl, *Nucl. Phys. B* **489**, 3 (1997) [hep-ph/9610370]; Z. Bern, L. Dixon and D. A. Kosower, *Nucl. Phys. B* **513**, 3 (1998) [hep-ph/9708239].
- [18] W. T. Giele, S. A. Keller and D. A. Kosower, arXiv:hep-ph/0104052.
- [19] J. Pumplin, D. R. Stump, J. Huston, H. L. Lai, P. Nadolsky and W. K. Tung, *JHEP* **0207**, 012 (2002) [arXiv:hep-ph/0201195].
- [20] S. Catani, L. Trentadue, G. Turnock and B. R. Webber, *Nucl. Phys. B* **407** (1993) 3.
- [21] A. Banfi and G. Zanderighi, private communication.